Point Processes for Interference Modeling in CSMA/CA Ad-Hoc Networks

Anthony Busson
University Paris-Sud 11
91405 Orsay Cedex, France
anthony.busson@u-psud.fr
Guillaume Chelius
University of Lyon, INRIA, ENS Lyon
ENS-Lyon, 69364 Lyon, France
guillaume.chelius@inria.fr

Abstract

As interference results from the summation of signals issued by concurrent transmitters, it directly depends on the transmitters location. The point process used to model concurrent transmitters location is thus fundamental in any multi-hop wireless network study. In this paper, we investigate original processes that comply with the CSMA/CA policies. We propose the use of the *Simple Sequential Inhibition* point process to model CSMA/CA networks where carrier detection depends on the strongest emitter only. We then extend this point process to a family of new point processes modeling a busy medium detection based on the strength of all concurrent signals. We study the impact of these different processes on the interference distribution and show that the results are very different with respect to the different point process. We finally show that the use of a Poisson process is generally inaccurate to model CSMA/CA networks.

I. Introduction

As interference plays a crucial role in ad hoc networks, these networks are often referred to as interference limited networks. Indeed, the network capacity is related to the radio channel reuse which is limited by the interference. In this paper we tackle the estimation of interference distribution in dense ad hoc networks. As interference results from the summation of signals issued by concurrent transmitters, it strongly depends on the transmitters location. The point process used to model nodes locations is thus fundamental in any study of such networks. In previous works, the spatial distribution of the radio nodes has generally been modeled thanks to a Poisson point process [4], [20], [8], [9], [10], [5]. However, the Poisson point process is accurate for very sparse networks only and suffers from a lack of realism in the case of dense networks. Indeed, it relies on the assumption that transmitters are independently distributed. In practice, the Medium Access Control protocol defines medium access rules to avoid collisions and by this way introduces a spatial correlation between the transmitters. Therefore, the spatial independence does not hold. Recent works [4], [13], [6] already tackle this problem by modifying the initial Poisson process according to the mechanisms of a CSMA/CA protocol. The initial Poisson point process is thinned to select effective transmitters by applying inhibition balls around all possible transmitters. This approach leads to the well known Matérn point process. However, as we will show in this paper, this approach suffers from two strong limitations. First, this approach tends to underestimate the number of concurrent transmitters and as a matter of fact, the interference level is strongly under-estimated in dense networks. Second, the thinning process assumes that a transmitter defers its transmission if it detects a busy medium due to the nearest previously selected transmitter. Albeit, medium access policies may rely either on carrier detection or on energy level. In the case of carrier detection, the inhibition model can be effectively related to the strongest signal, according to the Matérn selection process. However, in the case of energy detection, the candidate transmitter does not defer its transmission according to the strongest interference but rather to the interference level induced by all effective transmitters. In this case, the inhibition process is related to all concurrent transmitters and inhibition balls are not adequate.

In this paper, we investigate new original point processes to alleviate these limits and to better comply with CSMA/CA operating modes. Scenarios and assumptions are described in section II. Then, three point processes

are described in section III. First, the Matérn point process is described and built in a slightly different manner as usual. Then, the Simple Sequential Inhibition (SSI) point process introduced by Palásti [14] is described and its ability to model CSMA/CA networks is shown. Finally, we propose an extension of this SSI model to handle the CSMA energy detection mode.

In section IV, we evaluate the impact of the point processes on the interference properties. Albeit some analytical results are available for the Matérn process [18], [1], no analytical results are yet affordable for the SSI model. Therefore, our conclusions are drawn from simulation results. To fit with realistic assumptions, we have considered the parameters of a 802.15.4 868Mhz interface [16]. Mean interference level is first evaluated and the complete interference probability density functions are then drawn and compared to classical normal and log-normal distributions.

II. Models and scenarios

A. Interference modeling

When a single channel is shared by several nodes, interference is referred to as co-channel interference. For the sake of simplicity, we will restrict our work to the case of a single channel network, albeit the extension to multi-channel is obvious. Let us first introduce the radio reception level $S_j(x)$ at a position x of a signal emitted at x_j $S_j(x) = l\left(\|x - x_j\|\right) \cdot P_E$ P_E refers to the transmission power which we suppose constant for all nodes. $l(.)$ stands for the *path-loss* function which is related to the propagation model, and $\|.\|$ is the Euclidian norm. In most cases, $l(.)$ is a decreasing function from $\mathbb{R}^+$ in $\mathbb{R}^+$ that reflects the power decay with respect to the distance. In the simplest scenario, i.e. in line of sight (LOS), the path-loss is classically modeled using a power-law function derived from the Friis formula [15] : $l(u) = A_0 u^{-\beta}$ where A_0 is a constant related to physical parameters - antenna gains, free-space parameter - and $\beta = 2$ is the path-loss exponent. To avoid near field artifact, a more realistic model is obtained by bounding this function near 0. In the following, numerical simulations are obtained with $l(u) = min\left(1, \left(\frac{\lambda}{4\pi u}\right)^{\beta}\right)$ with $\beta > 2.0$ and λ the carrier wavelength. It is usual to consider the overall interference as a corruptive noise which affects the reception quality. In this case, the radio receiver performance is related to the Signal to Interference and Noise ratio (SINR) according to:

$$\Gamma_j(x) = \frac{S_j(x)}{N + I_\Phi(x)} \tag{1}$$

where N and I stand respectively for the receiver noise and the interference level. $I_\Phi(x)$ is equal to the sum of all interfering signals:

$$I_\Phi(x) \quad = \sum_{x_i \in \Phi; x_i \neq x_j} S_i(x) \tag{2}$$

where Φ is the set of concurrent transmitters. It should be noted that the radio link error probability can be directly derived from Equation 1 only if a linear receiver is used and if the interference behaves roughly like the receiver noise. This assumption may fail if the number of interferers is low or if it exists a single or few preeminent high power interferers. In this case, these strong interferers produce a correlated noise which affects in depth the performance of the receiver. If a medium access control (MAC) policy is used to prevent nearest interferers, this problem can be considered negligible.

B. Medium access control

The rules for assessing the radio medium are defined by the medium access control (MAC) protocol. In a CSMA/CA network, a candidate transmitter senses the channel before effectively transmitting. Depending on the channel state, clear or busy, the transmission is started or postponed. *Clear Channel Assessment* (CCA) depends on the MAC protocol and the terminal settings. For the two most widely used CSMA/CA protocols, IEEE 802.11 DCF and IEEE 802.15.4 [16], CCA is performed according to one of these three methods.

1) CCA Mode 1: *Energy above threshold.* CCA shall report a busy medium upon detecting any energy above the Energy Detection (ED) threshold. In this case the channel occupancy is related to the total interference

level $I_\Phi(x)$ (and possibly to any other radio system but let us keep this problem out of the scope of this paper).

2) CCA Mode 2: *Carrier sense only*. CCA shall report a busy medium only upon the detection of a signal compliant with its own standard, i.e. same physical layer (PHY) characteristics, such as modulation or spreading. In this case, this approach is rather sensitive to the highest interfering signal rather than the overall interference level. Note that depending on threshold values, this signal may be above or below the ED threshold.
3) CCA Mode 3: *Carrier sense with energy above threshold.* CCA shall report a busy medium using a logical combination (e.g. AND or OR) of Detection of a compliant signal AND/OR Energy above the ED threshold.

A common consequence of the CSMA/CA modes is that two transmitters cannot be very closed to each other. Note that the Poisson point process does not take into account this constraint and thus leads to a large inaccuracy in the distribution of emitters for a CSMA/CA network.

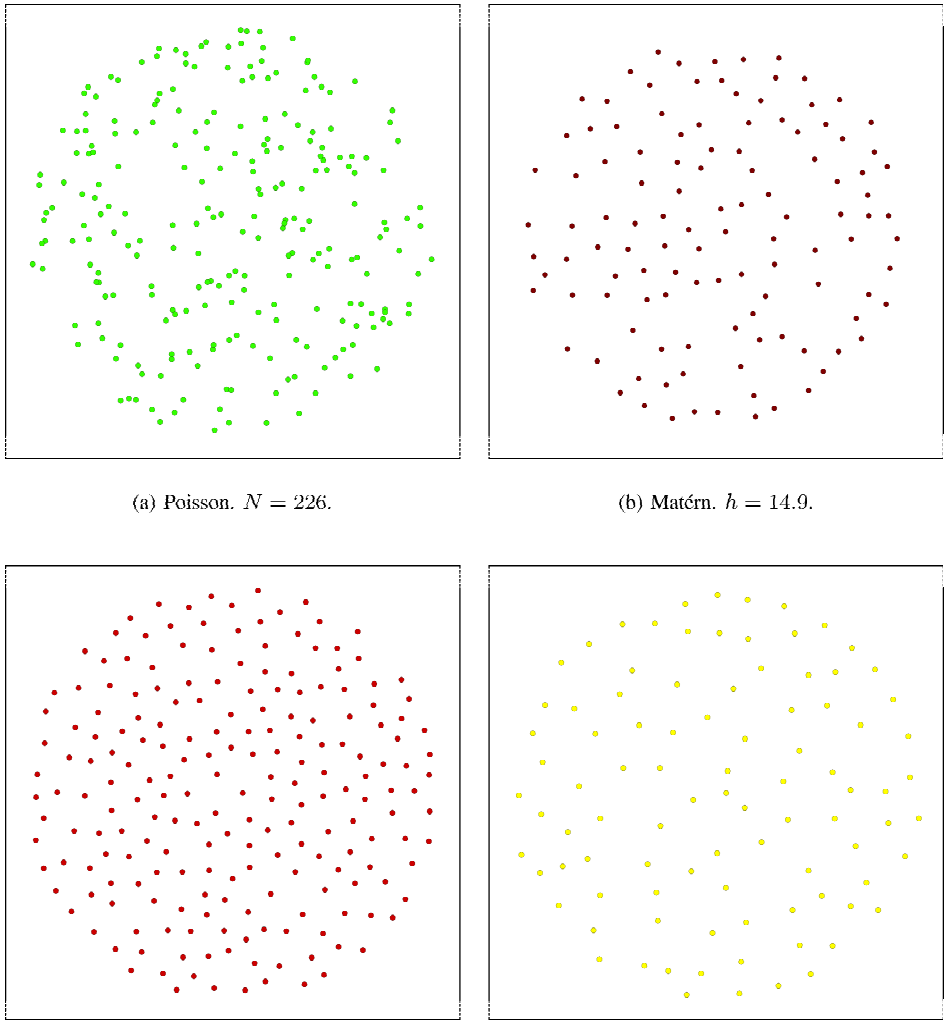

(a) Poisson. $N = 226$.

(b) Matérn. $h = 14.9$.

(c) SSI. $h = 14.9$.

(d) SSI_N. See Table I for the parameters.

Fig. 1. Samples of the different point processes. For all the point processes except the Poisson one, we consider scenario 1 with $R = 150.0$. $N = 1500$.

C. Scenarios

We consider the transmission of a frame between an emitter, denoted Y, and a receiver located at the origin O and denoted X_0. The interference distribution is evaluated for this node, *i.e.* at the origin. Further, the following assumptions are assumed.

1) Let R_{inh} be the inhibition radius defined as the distance for which the signal strength of an emission is equal to the Energy Detection threshold (ED) denoted θ. It is defined according to $\theta = l(R_{inh}) \cdot P_E$.
2) Without lack of generality and when not otherwise stated, the emitter Y is located at a distance $\frac{R_{inh}}{2}$.

Four scenarios with the following features are considered:

1) The first scenario stands for the reference case. No RTS/CTS is used. Y has sensed the medium clear and transmits data. Therefore potential transmitters in the vicinity of the transmitter are kept off. The interference at origin is computed as the sum of interfering signals generated by all transmitters except Y. Let Φ be the point process modeling the set of interfering nodes, one gets:

$$I_\Phi(O) = \sum_{X_i \in \Phi} P_E l(\|X_i\|) \tag{3}$$

2) Scenario 2 models a transmission with RTS/CTS. The RTS/CTS mechanism is introduced in the point process model by considering that the receiver at the origin has also sensed a clear medium before the transmission and has transmitted a CTS. Therefore potential transmitters in the vicinity of the transmitter and the receiver are kept off. Thus, the emitter selection process differs from the first scenario but the final computation of interference still relies on (3).
3) Scenario 3 derives from scenario 1 (without RTS/CTS) but considering that X_0 has the capability to cancel the highest interfering signal thanks to a multi user detection (MUD) receiver. Therefore, the preponderant interfering node which is the closest to the origin is neglected in the interference computation:

$$I_\Phi(O) = \sum_{X_i \in \Phi, X_i \neq X_1} P_E l(\|X_i\|)$$

where X_1 is the closest interferer to the origin. Note however that this node is taken into account during the selection of concurrent transmitters.
4) Scenario 4 extends scenario 2 (with RTS/CTS) to the case of a MUD receiver, i.e. X_0 having the capability to cancel the highest interfering signal.

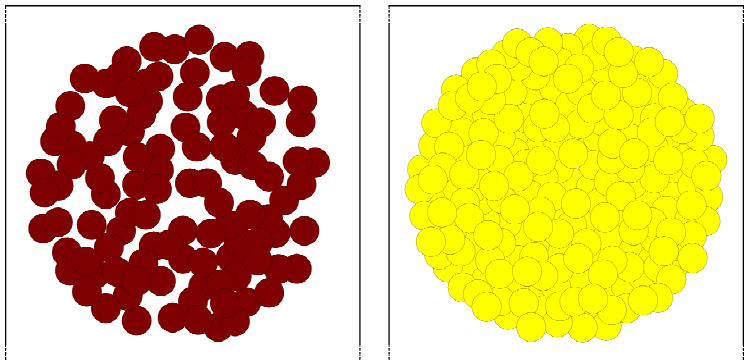

(a) Sample of a Matérn point process with its active inhibition balls.

(b) Sample of a SSI point process with its inhibition balls.

Fig. 2. Samples of Matérn and SSI point processes with the inhibition balls of the active transmitters. Scenario 1, $R = 150.0$, $N = 1500$ and $h = 14.9$.

III. Point processes

In this Section, we present the different point processes used to model the spatial distribution of concurrent transmitters.

A. Poisson point process

Let us first consider the classical Poisson point process. A deep presentation of this point process can be found in [7], [18]. A sample of this point process is plotted in Figure 1(a). This process has been extensively used to model spatial distributions of active transmitters in *ad hoc* networks [4], [20], [8], [9], [10], [5]. One reason for this popularity is certainly the tractability of the interference distribution which is unaffordable for many other point processes. For instance, the Laplace transform of the interference distribution can be assessed, and the *frame error rate* (*FER*) can be deduced for some special cases [4]. However, the Poisson point process is only suitable to model sparse networks where transmitters can be assumed uncorrelated. In contrary, for dense networks using a CSMA/CA protocol, the MAC protocol introduces a correlation between the active transmitters location. As we will show in next section, the Poisson point process leads in fact to a very different interference distribution compared to the ones obtained with more realistic point processes. The Matérn point process presented hereafter is used to capture in some part the mechanisms of the CSMA/CA protocol.

B. Matérn point process

The Matérn point process belongs to the family of *hard-core* point processes, where points are forbidden to lie closer to each others than a certain distance h ($h > 0$). The Matérn point process was introduced in [2], [3] and a convenient presentation can also be found in [18]. The Matérn point process is a dependent thinning of a Poisson point process. Thus, the set of radio nodes who stand for possible transmitters follows a Poisson point process while the distribution of instantaneous effective transmitters is modeled by a Matérn process. In the classical approach, the points of the underlying Poisson point process are deleted in such a way that the remaining points are distant of at least h. Thus, the minimal distance h between active nodes stands for the maximal distance at which a node detects a compliant signal (CCA Mode 2). If the signal strength received from the closest neighbor is less than ED θ, the transmission starts; otherwise it is deferred. Therefore, in numerical evaluations, the value h corresponds to the inhibition radius R_{inh} defined in Section II-C.

In this paper, we propose a slightly different description of the classical Matérn point process. While in the original point process, the selection process is function of random marks associated to each point, we propose here to use a selection process that depends on the arrival order of the points. Moreover, according to the scenarios described in Section II, we locate first Y (Scenario 1 and 3) or (Y, X_0) when the RTS/CTS mechanism is used (Scenarios 2 and 4). Then the point process is built as follows:

- Let N be a positive integer and let $\Phi_M(i)$ be the set of points selected after i steps. $\Phi_M(0) = \{Y\}$ for scenarios 1 and 3, and $\Phi_M(0) = \{Y, X_0\}$ for scenarios 2 and 4.
- Let $(X_i)_{1 \leq i \leq N}$ be a sequence of random variables uniformly distributed in $B(0, R)$. The Matérn process $\Phi_M(N)$ is built for $i \in [1, N]$ according to:

$$X_i \in \Phi_M(i+1) \text{ iif } \|X_i - Z\| > R_{inh} \forall Z \in \Phi_M(i)$$

In other words, at each step, a new emitter attempts acquiring the medium. If its distance to all other points is greater than R_{inh}, it succeeds. Otherwise the new point is kept inactive. Note however that this inactive emitter is anyway considered in the selection process of the following points. It is worth noting that the selection of a new point as active emitter depends on all previous points, even the inactive ones. A sample of this point process is plotted in Figure 1(b) while Figure 2(a) depicts a sample of the inhibition balls associated with a set of active transmitters selected through a Matérn point process with $N = 1500$. For this value of N, the point process reaches saturation, *i.e.* no further active transmitter can be added. This figure clearly shows that even with N tending to infinity, some areas remain clear of active transmitters due to the presence of inactive but inhibiting points. This observation illustrates a spatial anomaly of the Matérn process related to the fact that inactive points nevertheless impact the selection process. In the next Section, a Hard Core point process is introduced to deal with this spatial anomaly. In this alternate process, the selection of a new point depends only on points previously selected as active transmitters.

C. Simple Sequential Inhibition (SSI)

The SSI point process was introduced by Palásti [14] and appears to be more appropriate to model CSMA/CA networks. This model belongs to a family of well-known models used in the context of *packing* or *space filling problems*. They are concerned with the distribution of *solids* in k-dimensional spaces [11], [17]. The point process $\Phi_S(N)$ is built as follows:

- Let N be a positive integer and let $\Phi_S(i)$ be the set of points selected in the SSI after i steps ($\Phi_S(0) = \Phi_M(0)$).
- Let $(X_i)_{1 \leq i \leq N}$ be a sequence of random variables uniformly distributed in $B(0, R)$. The SSI process is built for $i \in [1, N]$ according to:

$$X_i \in \Phi_S(i+1) \text{ iif } \|X_i - Z\| > R_{inh} \forall Z \in \Phi_S(i)$$

In other words, at each step, a new emitter attempts to acquiring the medium. If its distance to all actual active emitters is greater than R_{inh}, it becomes active. Otherwise, this emitter is kept off, deleted from the transmitter list and is no longer considered in the selection process. A sample of this point process is plotted in Figure 1(c). The transmitter spatial distribution appears to be more regular than the Poisson one. Indeed, clusters of adjacent transmitters are avoided. Furthermore, the spatial distribution appears also to be more regular than the Matérn one. The problem of clear areas is avoided. This result is clearly observed in Figure 2(b) where the inhibition balls associated with the SSI point process are depicted. Contrarily to the Matérn point process, the inhibition balls cover the whole observation window. The SSI process thus offers a better way to model CSMA based networks implementing CCA Mode 2 described in section II. However, in this approach, a static inhibition ball is still used and CCA Mode 1 can hardly be modeled. In this case, the detection threshold is compared to the interference level induced by all emitters and not only the strongest one. With this process, we can hardly handle the additive nature of interference. The next model intends to address this issue.

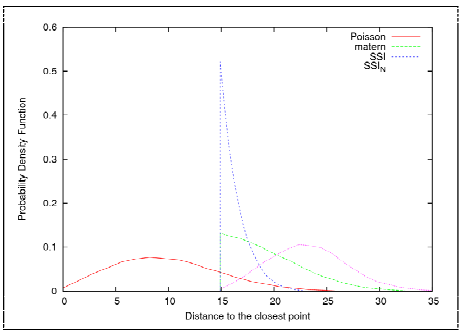

(a) Distribution of the closest interferer.

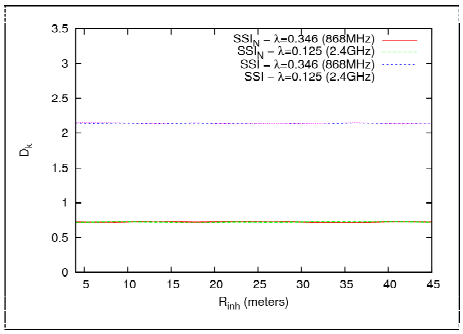

(b) D_k.

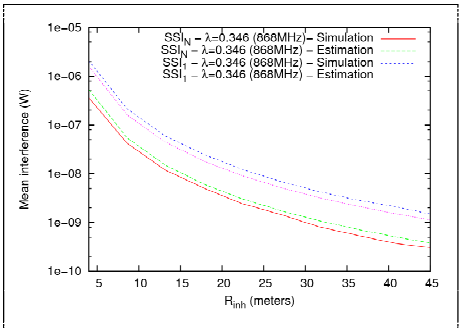

(c) Mean interference estimations.

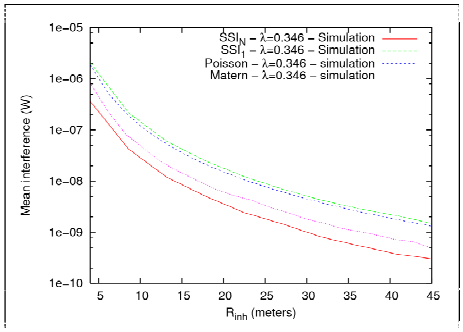

(d) Mean interference.

Fig. 3. Distribution of the closest interferer for the different point processes and mean interference estimations vs simulations.

D. An extension to the Simple Sequential Inhibition (SSI_k)

We propose an extension to the SSI model denoted SSI_k. It considers the interference level generated by the k-closest neighbors in the selection process rather than the closest one only. The process is built as follows:

- Let N and k be two positive integers. Let θ be the detection threshold and $\Phi_{S_k}(i)$ be the set of points selected in the SSI_k after i steps ($\Phi_{S_k}(0) = \Phi_M(0)$).
- Let $(X_i)_{1 \leq i \leq N}$ be a sequence of random variables uniformly distributed in $B(0, R)$. The SSI_k process is built for $i \in [1, N]$ according to:

$$X_i \in \Phi_{S_k}(i+1) \text{ iif } \sum_{j=1}^{k} l(\|X_i - Y_j\|) \cdot P_E < \theta \forall Y_j \in \Phi_{S_k}(i)$$

with $l(\|X_i - Y_1\|) < l(\|X_i - Y_2\|) < \cdots < l(\|X_i - Y_k\|)$.

In other words, at each step, a new emitter attempts to acquiring the medium. If the interference generated by the k closest emitters is less than the detection threshold θ, the transmitter becomes active. Otherwise, the new point is deleted and no longer considered in the selection process. Note that if $k = N$, all the active emitters are considered when computing the interference level.
A sample of this point process, for $k = N$, is plotted in Figures 1(d). In the rest of this paper, we shall always consider the hard-core point process with $N \to +\infty$. It describes the saturated case, where no further active emitter can be added.

It is worth noting that some emitters may suffer from an interference level greater than θ at the end of the selection process. Indeed, albeit the interference level of a new emitter X_i is bounded by θ, its interference can be increased later by the selection of new transmitters $X_j; j > i$. Note however that this phenomena is closed to the real behavior of CSMA/CA protocols as interference is measured spatially and temporally without considering the interference increase that could result from later transmitters.

E. Transmitter spatial distributions

Figure 3(a) depicts the distribution of the distance between a randomly chosen point of the point process in $B(0, \frac{R}{2})$, and its closest active neighbor. It assesses the distance distribution between an emitter and its closest interferer. These distributions have been obtained by simulations. In order to avoid edge effects, the point processes are scattered in a larger window $B(0, R)$. The set of parameters are given in Table I. It appears clearly that the Poisson point processes leads to a very different distribution, where the points can be very close to each others compared to the other point processes. It seems clear that these differences should have an important impact on the radio properties. In the next Section, we evaluate the impact of these point processes on the interference level.

IV. Interference

In the previous section, different approaches have been proposed to thin a Poisson process according to the CSMA/CA modes. We have observed how the spatial distribution of simultaneous emitters may be influenced by these rules. In this section, we investigate how these point processes may lead to different interference statistics.

802.15.4 868MHz Parameters	Numerical Values	Simulation parameters	Numerical values
Frequency	868MHz	R	100.0 meters
Wavelength	0.346 meters	Radius of inhibition	14.9 meters
Energy Detection Threshold (θ)	$6.309573e^{-12}$ Watts	N (except for Poisson)	1500
Emission power	0.001 Watts	Number of samples	at least 200, 000
β (path-loss parameter)	3.0		

TABLE I
Simulation parameters.

A. Point process intensity

We first investigate the transmitter intensity μ according to the modified Matérn and SSI point processes. The modified Matérn point process intensity μ is equal to the one of the classical Matérn process with an underlying Poisson process intensity tending to infinity. Thus, one have $\mu \approx \frac{1}{\pi R_{inh}^2}$ ([18]). For the SSI, it has been conjectured in [14], that

$$\lim_{R,N\to+\infty} \frac{N_{SSI} \cdot R_{inh}^2}{R^2} = 4 \cdot c \tag{4}$$

where N_{SSI} is the number of points of the SSI in $B(O,R)$ and c is a constant later approximated to $c \simeq 0.56$ [19], [12]. For our proposed point processes SSI_k, we have evaluated the validity of Equation (4) with a specific value of c. Let us write $D_k = \lim_{N,R\to\infty} \frac{\mathbb{E}[N_{SSI_k}] R_{inh}^2}{R^2}$ for large R and N, where R_{inh} equals the one of the SSI process. We use simulation results to evaluate the accuracy of this approximation. To comply with realistic assumptions, parameters are set according to the 802.15.4 standard. D_k is plotted in Figure 3(b) with R_{inh} varying from 4 to 45 meters - θ varying from $3.2e-07dB$ to $2.3e-10dB$ - and for $\beta = 3$. In these plots, D_k appears constant for all test sets. For SSI_N, we find $D_N = 0.72$. As a consequence, these simulations show that we can experimentally estimate the intensity of the SSI_k point process as $\mu_k = \frac{D_k}{\pi R_{inh}^2}$.

B. First moment of interference distribution

We now investigate the first moment of the interference distribution. We evaluate it as:

$$\mathbb{E}\left[I_\Phi(O)\right] = \mu \int_\Omega l\left(\|x\|\right) dx \tag{5}$$

with Ω the observation area where emitters are distributed. $\Omega = B(O,R) \setminus B(Y, R_{inh})$ for scenarios 1 and 3, $\Omega = B(O,R) \setminus (B(Y,R_{inh}) \cup B(O,R_{inh}))$ for scenarios 2 and 4.

For the modified Matérn and SSI processes, formula 5 only offers an approximation as stationarity does not hold formally. An exact formula was found in [1] for the modified Matérn point process. We propose instead to use the above expression as an approximation of the true expression. We further extend this approximation to the SSI family. It follows that the mean interference value relies on the average path-loss over Ω and on the point process intensity μ. Therefore, The problem boils down to the estimation of μ which was studied in the previous section.

The mean interference for Scenario 1 is plotted in Figure 3(c) as a function of R_{inh} (or equivalently function of θ). The difference between the simulation curves and our proposed approximation is tight. It validates the approximation proposed by formula 5. We can guess that the small difference is probably due to edge effects introduced by the presence of Y and the boundary of $B(O,R)$.

In figure 3(d), we plot the mean interference for the four point processes. As expected, SSI and Poisson coincide as they have the same intensity. For the two other point processes, we observe a significant difference.

C. Interference pdf

In the previous section, we have derived an approximation of the mean interference level for different scenarios. However, this mean interference level is not representative of the performance of the radio transmissions. Indeed, the complete interference distribution may impact the performance of a receiver. In this Section, we present the *probability density functions* (*pdf*) of interference at the origin as obtained with the different point processes and scenarios. These *pdf* are assessed by simulations and we do not derive any analytical expression. For all the point processes, except for the Poisson one, the number of potential emitters N is chosen such that no more active emitters can be added to the point process, *i.e.* after saturation. For the Poisson point process, the intensity is chosen equal to the one of the SSI_1. Such configurations correspond to dense networks where a high number of nodes compete for the medium.

As described above, the simulation parameters are set according to the IEEE 802.15.4 standard [16]. For the sake of compactness, only the results corresponding to the 868MHz band are herein provided. Note however that the conclusions are similar for the $2.4GHz$ band. The set of parameters is given in table I.

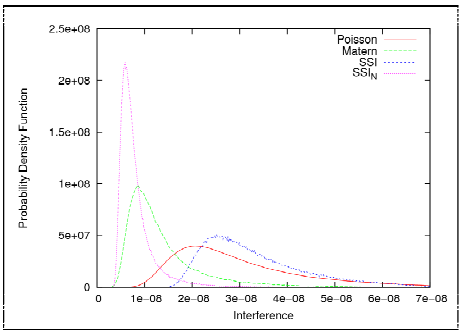

(a) Scenario 1.

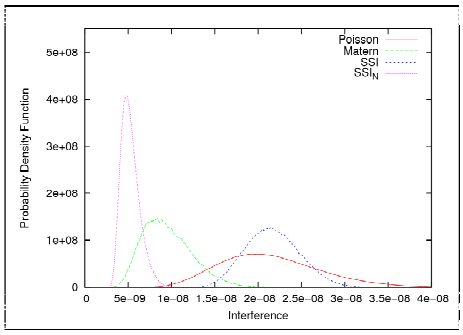

(b) Scenario 2.

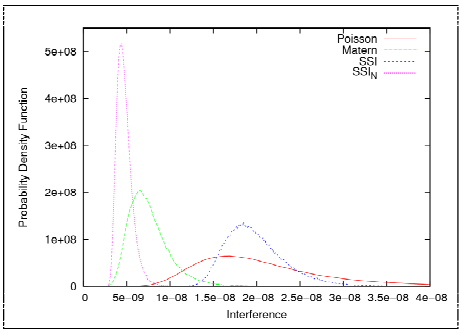

(c) Scenario 3.

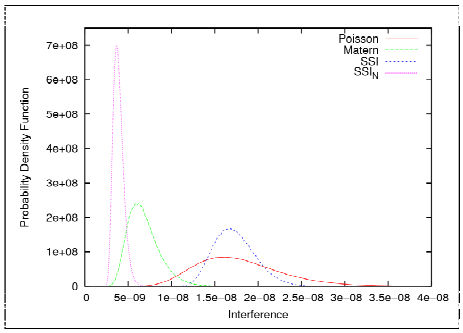

(d) Scenario 4.

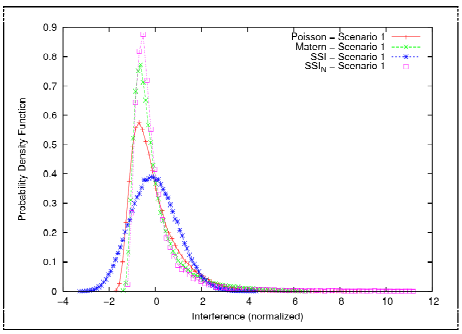

(e) Scenario 1.

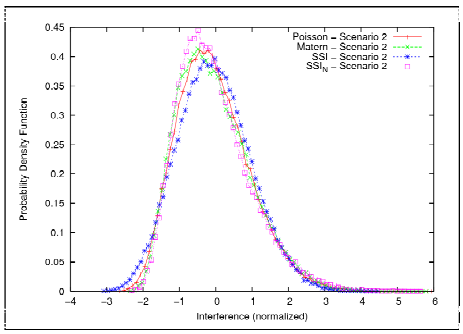

(f) Scenario 2.

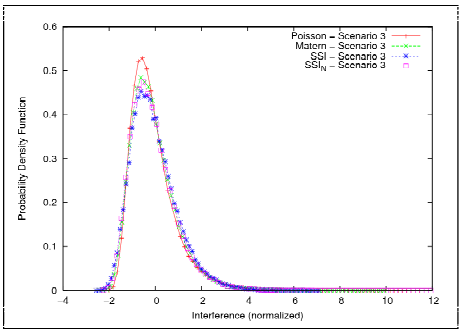

(g) Scenario 3.

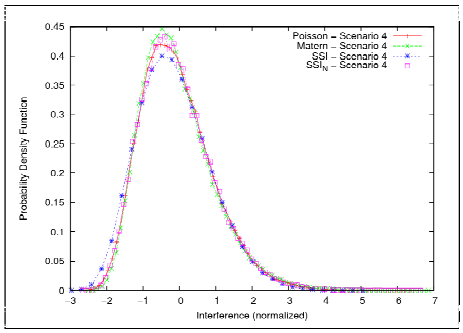

(h) Scenario 4.

Fig. 4. For a given scenario, comparison of interference *pdf* between the point processes. In Figures 4(e) to 4(h), the samples have been normalized.

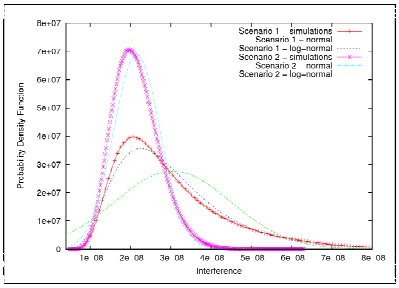

(a) Poisson - Scenarios 1 and 2.

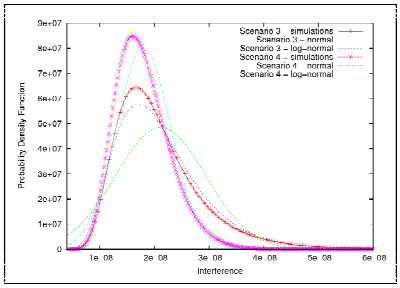

(b) Poisson - Scenarios 3 and 4.

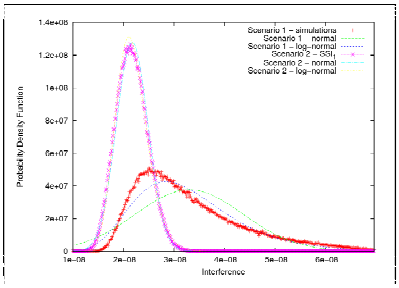

(c) SSI - Scenarios 1 and 2.

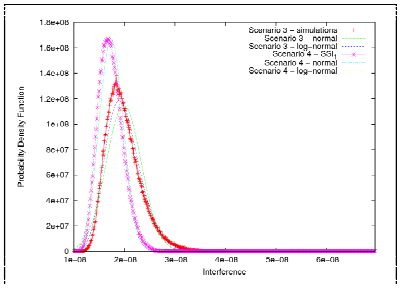

(d) SSI - Scenarios 3 and 4.

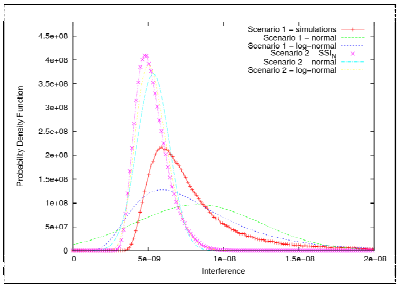

(e) SSI_N - Scenarios 1 and 2.

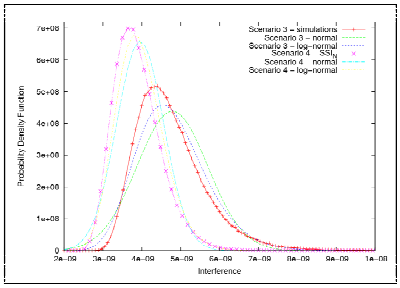

(f) SSI_N - Scenarios 3 and 4.

Fig. 5. Comparison of interference *pdf* with normal and log-normal distributions.

a) Comparison between the point processes: In Figures 4(a) to 4(d), we compare the interference *pdfs* for the 4 point processes and for the four scenarios. As we can see, the various point processes offer largely different interference *pdfs* though they all offer the same global shape: a peak and an asymmetry with a more or less heavy tail depending on the point process. The main reason for which the *pdfs* seem to follow different distributions is that they offer different means and variances. In order to verify that they do not belong to the same family of distributions, we compare these *pdfs* again after normalizing the samples. More precisely, for the set of samples $(x_i)_{i\leq n}$ corresponding to a point process, we evaluate the distribution of $(x_i^{'})_{i\leq n}$ with $x_i^{'} = \frac{x_i - m}{\sqrt{v}}$, $m = \frac{1}{n}\sum_{i=1}^{n} x_i$ and $v = \left(\frac{1}{n}\sum_{i=1}^{n} x_i^2\right) - m^2$. The normalized distributions are plotted in Figures 4(e) to 4(h). For scenario 1, the distributions are clearly different. For the three other scenarios, the *pdfs* are very close to each others. Indeed, as we shall show, for these scenarios, the different distributions get close to a log-normal distribution. In consequence, a normalization of the samples leads logically to distributions which offer a good similarity to a log-normal distribution with mean 0 and variance 1. However, a sequence of Smirnov-Kolmogorov tests with 5% significance level rejects

the assumption that they follow the same distribution.

b) Comparison with normal and log-normal distributions: In Figures 5(a) to 5(f), we compare the interference *pdf* with normal and log-normal distributions. By lack of place, we plot only the interference *pdf* for the Poisson, SSI and SSI_N point processes. We have also performed two hypothesis tests, a χ^2 and a Smirnov-Kolmogorov tests with 0.05 significance level. The tests lead to the reject of the *null* assumption, *i.e.* interference is normally or log-normally distributed for all point processes and scenarios. Nevertheless, the χ^2 and Smirnov-Kolmogorov statistics allow us to objectively compare the accuracy of the normal or log-normal approximations. And the two tests have systematically agreed on the choice of the better approximation. It is clear, that for scenario 1, neither normal and log-normal distributions fit, even if the log-normal one offers a better approximation. For the other scenarios, the two distributions fit very well. According to the statistics of the hypothesis tests, the log-normal is, for most of the point processes, the best approximation. The exception is for the SSI scenario 2, where the interference *pdf* is closer to a normal distribution.

We also made hypothesis tests for other sets of parameters ($\beta = 2.0$ and 4.0 for the $868MHz$ band and $\beta = 2.0, 3.0$ and 4.0 for the $2.4GHz$ band). The results are qualitatively the same: log-normal distribution fits the interference distribution very well except for scenario 1.

c) Discussion: It clearly appears that for scenario 1, the Poisson point process cannot be used to model CSMA/CA networks as it leads to a very different interference distribution with regard to more realistic point processes. For scenarios 2, 3 and 4, the four point processes lead to interference *pdfs* of the same distribution family, close to a log-normal distribution. However, several factors justify the use of a SSI_k point process rather than a Poisson one for these scenarios. First, the intensity of active transmitters can hardly be guessed with a Poisson point process whereas it is provided by saturation for SS_k point processes. Second, even for a common intensity of active transmitters, the interference variance obtained with a Poisson point process is two or three times greater than the one obtained with the SSI family.

V. Conclusion

In this article, we have proposed to use the SSI point process in order to better model the spatial distribution of active transmitters in CSMA/CA based wireless multi-hop networks. We have also extended this particular point process to a new family of hard-core point processes, SSI_k, in order to comply with the different CSMA/CA operating modes. The SSI point process can be used to model a network where the medium is sensed busy upon detection of a compliant signal whereas SSI_k processes can be used when the medium is sensed busy depending on the interference energy level, considering all interfering signals.

A deep study of the interference clearly shows that the use of various point processes lead to largely different distributions. When the RTS/CTS mechanism is not triggered, it seems that the interference distributions can hardly be extrapolated using any well-known law, whichever the underlying point process. However, when the RTS/CTS mechanism is triggered, the interference distribution get similar to a log-normal law.

However, even under this condition, the Poisson point process fails to correctly model active transmitters. For example, it does not provide any information on the transmitter intensity whereas hard-core processes do so after reaching the saturated case. And even if we set artificially the intensity of the Poisson point process, we get unrealistic variances. If the Matérn point process seems more realistic, it still suffers flaws such as the spatial anomaly and thus an under-estimation of the interference level. Ultimately, the SSI_k point process family seems the most suited to offer a realistic modeling of the different operating modes of CSMA/CA based ad hoc networks.

References

[1] J.-M. A. Busson, G. Chelius and Gorce. Interference modeling in csma multi-hop wireless networks. Research Report RR-6624, INRIA, Sept. 2008.

[2] M. B. Spatial variation. *Meddelanden fran Statens Skogsforskningsinstitut*, 49(5):1–144, 1960.

[3] M. B. Spatial variation. *Lecture Notes in Statistic 36. Springer Verlag, Berlin, Heidelberg, New York*, 1986.

[4] F. Baccelli, B. Błaszczyszyn, and P. Mühlethaler. An aloha protocol for multihop mobile wireless networks. *IEEE Transactions on Information Theory*, 52(2):421–436, 2006.

[5] E. Ben Hamida, G. Chelius, A. Busson, and E. Fleury. Neighbor discover in multi-hop wireless networks: evaluation and dimensioning with interference considerations. *Discrete Mathematics and Theoretical Computer Science*, 10(2):87–14, 2008.

[6] T. Cheng, Y.-C.; Robertazzi. A new spatial point process for multihop radio network modeling. In *SUPERCOMM/ICC*, 1990.

[7] D. Daley and D. Vere-Jones. *An Introduction to the theory of point processes.* Springer-Verlag, New York, USA, 2003.

[8] O. Dousse, F. Baccelli, and P. Thiran. Impact of interferences on connectivity in ad hoc networks. *IEEE/ACM Transactions on Networking*, 13(2):425–436, Apr. 2005.
[9] O. Dousse, P. Thiran, and M. Hasler. Connectivity in ad-hoc and hybrid networks. In *Conference on Computer Communications (INFOCOM)*, New York, USA, June 2002. IEEE.
[10] P. Gupta and P. Kumar. Capacity of wireless networks. *IEEE Transactions on Information Theory*, 46(2):388–404, 2000.
[11] P. Hall. *Introduction To the Theory of Coverage Processes*. Wiley, 1988.
[12] H. W. Lotwick. Simulations of some spatial hard-core models, and the complete packing problems. *Journal of Statistical Computation and Simulation*, 15:295–314, 1982.
[13] H. Nguyen, F. Baccelli, and D. Kofman. A stochastic geometry analysis of dense ieee 802.11 networks. In *Conference on Computer Communications (INFOCOM)*, Anchorage, USA, May 2007. IEEE.
[14] I. Palasti. On some random space filling problem. *Publications of Mathematical Institute of Hungarian Academy of Sciences*, 5(1):353–359, 1960.
[15] S. Saunders. *Antennas and propagation for wireless communication systems*. Wiley, 1999.
[16] I. C. Society. Ieee standard for information technology - telecommunications and information exchange between systems - local and metropolitan area networks - specific requirements - part 15.4: Wireless medium access control (mac) and physical layer (phy) specifications for low-rate wireless personal area networks (wpans). Technical report, IEEE Computer Society, 2006.
[17] H. Solomon and H. Weiner. A review of the packing problem. *Communications in Statistics and Theoretical Methods*, 15:2571–2607, 1986.
[18] D. Stoyan, W. Kendall, and J. Mecke. *Stochastic Geometry and Its Applications, 2nd Edition*. John Wiley and Sons Ltd, Chichester, UK, 1996.
[19] M. Tanemura. On random complete packing by disks. *Annals of the Institute of Statistical Mathematics (AISM)*, 31:351–365, 1979.
[20] X. Yang and A. P. Petropulu. Co-channel interference modeling and analysis in a poisson field of interferers in wireless communications. *IEEE Transactions on Signal Processing*, 51(1):64–76, Jan. 2003.